

# Photoluminescence Properties of Copolyimides Containing Naphthalene Core and Analysis of Excitation Energy Transfer between the Dianhydride Moieties

Marina Doi<sup>1</sup>, Koichiro Muto<sup>1</sup>, Mayuko Nara<sup>1</sup>, Naiqiang Liang<sup>1</sup>, Kosuke Sano<sup>2</sup>, Hiroaki Mori<sup>2</sup>, Ryohei Ishige<sup>1</sup>, and Shinji Ando<sup>1\*</sup>

<sup>1</sup> Department of Chemical Science and Engineering, Tokyo Institute of Technology, Ookayama, 2-12-1-E4-5, Meguro-ku, Tokyo 152-8552, Japan

<sup>2</sup> Chemical Research Laboratory, JFE Chemical Corporation, Kawasaki-cho, 1, Chuo-ku, Chiba-shi, Chiba 260-0835, Japan

\*ando.s.aa@m.titech.ac.jp

The photoluminescence (PL) properties of semi-aromatic polyimide (PI) films and their model compounds (MCs) prepared from dianhydrides having a rigid naphthalene core were analyzed. The PMMA-dispersed MC and copolymerized PI (CoPI) films derived from 2,3,6,7-naphthalenetetracarboxylic dianhydride (NTDA) exhibited long-lived phosphorescence owing to the suppression of molecular motion by the rigidity of a naphthalene core. Additionally, the PMMA-dispersed MC and the CoPI films derived from 1,5-dibromo derivative of NTDA (DBrNT) exhibited room-temperature phosphorescence due to the enhancement of spin-orbit coupling by bromine atoms. The photophysical processes of the CoPI films prepared from NTDA/DBrNT and 4,4'-oxydiphtalic dianhydride (ODPA) in which the latter absorption band is located at a shorter wavelength than the former were analyzed. After UV irradiation, efficient excitation energy transfer occurs from the ODPA to NTDA/DBrNT moieties, and only the emission from the latter moieties was observed. These results demonstrate that the CoPI films derived from two dianhydrides absorbing different UV wavelengths can be used as spectral conversion films that convert a wide range of UV-light into longer wavelength visible light.

**Keywords:** Polyimide, Copolymer, Naphthalene, Energy transfer, Spectral conversion

## 1. Introduction

Polyimides (PIs) are a class of super engineering plastics, and they are widely used for their high thermal, environmental, and radiation stabilities, originating from their rigid repeating unit structures and strong intermolecular interactions [1–2]. Therefore, PIs have been applied in numerous fields, including automotive, microelectronic, photonic, electronic, and aerospace industries. Owing to their characteristic photoluminescence (PL) properties and excellent performance, PI films have been extensively studied as novel thermally stable photoluminescent materials [3–11].

The present authors recently reported a novel white-light emitting PI film by copolymerizing a

fluorescent and a phosphorescent PIs [5,12]. Moreover, we have also reported that, by introducing heavy halogens, iodine and bromine, into the dianhydride moiety of PIs, bright phosphorescence (Ph) can be observed at room temperature owing to the heavy atom effect [13,14]. This effect is a phenomenon that introduction of metal or heavy halogen into organic fluorophores enhances the spin-orbit coupling (SOC) interactions and promotes the inter-system crossing (ISC) between the excited singlet and triplet states, which is generally forbidden [15,16]. Room temperature Ph has been expected to be applied to bioimaging [17], document security [18], and wavelength conversion films [19] because it generally exhibits

an emission at longer wavelengths accompanied by a much longer emission lifetime than fluorescence (Fl) [20,21]. It has been reported that the Ph intensity can be significantly increased at lower temperatures (e.g. 77 K) due to the suppression of local molecular motion [13]. This is because the contribution of non-radiative deactivation induced by local molecular motion is more significant in the Ph processes than in Fl due to the long lifetime of triplet excitons [22–26]. It has been difficult to develop organic compounds that exhibit long-lived Ph at room temperature and in air because Ph is easily quenched by molecular motion at higher temperatures and triplet oxygen in air. In recent years, however, it is strongly in demand to develop organic phosphorescent materials which exhibit long-lived Ph at room temperature, from the perspective of reducing costs and environmental impact. For this reason, the development of organic long-life phosphorescent materials is now being actively pursued [27,28]. In addition, crystalline and multi-crystalline silicon (Si) solar cells, which are mainly used in practical applications, have low absorption coefficients and poor spectral sensitivity to sunlight in the ultraviolet (UV) region [29]. Therefore, phosphorescent materials exhibiting emissions at longer wavelengths than fluorescent materials are expected to be used as spectral conversion films that convert the UV light to the visible light in the longer wavelength range, in which Si solar cells have much higher spectral sensitivity [30].

In this study, we mainly focused on the suppression of molecular motion by introducing a rigid aromatic structure. It is expected that the phosphorescent properties of the PIs derived from dianhydrides having an enlarged  $\pi$ -conjugated

system can be improved due to the suppression of molecular motion by strong intermolecular  $\pi$ - $\pi$  stacking. In that sense, the PIs having a rigid naphthalene core in the dianhydride moiety are expected to undergo restricted molecular motion due to the well-packed  $\pi$ -conjugated system in the solid state. Firstly, we synthesized imide model compounds and PIs using 2,3,6,7-Naphthalenetetracarboxylic dianhydride (NTDA) and evaluated their phosphorescent properties. We also synthesized copolymerized PIs (CoPIs) using NTDA and another dianhydride which absorbs UV light at a different wavelength and investigated the efficiency of energy transfer in the excited states between the dianhydrides.

## 2. Experimental

### 2.1. Materials.

2,3,6,7-Naphthalenetetracarboxylic dianhydride (NTDA), 4,4'-(hexafluoroisopropylidene) diphthalic anhydride (6FDA) and 4,4'-oxydiphthalic anhydride (ODPA) were kindly supplied by JFE Chemical Co. (Tokyo, Japan), NTT Advanced Technology Co. (Tokyo, Japan), and MANAC Inc. (Tokyo, Japan) respectively. They were purified by drying at 150 °C for 5 h in vacuo followed by sublimation under reduced pressure. 1,5-Dibromo-2,3,6,7-naphthalene tetracarboxylic dianhydride (DBrNT) was synthesized and supplied by JFE Chemical Co. (Tokyo, Japan). Cyclohexylamine (CHA) purchased from Kanto Chemical Co. (Tokyo, Japan), *N,O*-Bis(trimethylsilyl) trifluoroacetamide (BSTFA), polymethyl methacrylate (PMMA), and *N,N*-dimethyl acetamide (anhydrous, 99.8%, DMAc) from Sigma-Aldrich Japan (Tokyo, Japan), chloroform from Wako Pure Chemical Industries,

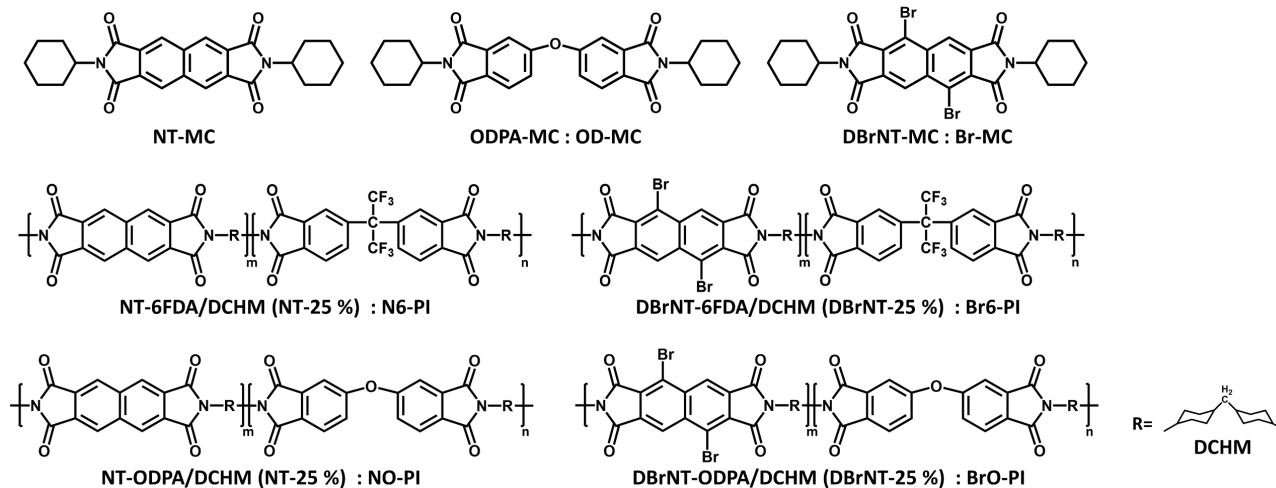


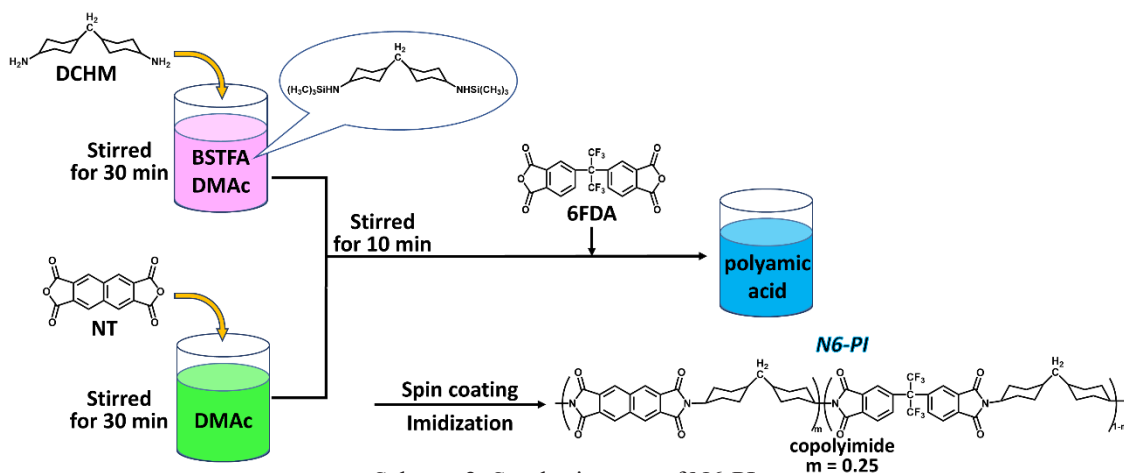
Chart 1. Chemical structures of imide compounds (MCs) and CoPIs.

Ltd. (Osaka, Japan), trifluoroacetic acid (TFA) from Tokyo Kasei Kogyo Co. Ltd. (Tokyo, Japan), and propionic acid from Kanto Chemical Co. (Tokyo, Japan) were used without further purification. Diaminodicyclohexylmethane (DCHM) from Tokyo Kasei Kogyo Co. Ltd. (Tokyo, Japan) was purified by recrystallization from *n*-hexane, followed by sublimation under reduced pressure.

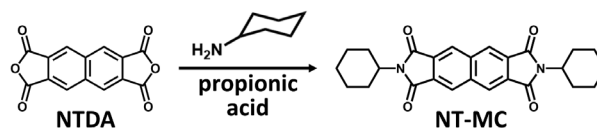
## 2.2. Synthesis and film preparation of imide model compounds (MCs).

The synthesis scheme of an imide model compound (NT-MC) is shown in Scheme 1. CHA (1.5 g, 15 mmol) and NTDA (1.26 g, 4.7 mmol) were stirred in propionic acid (25 mL) for 30 min. The solution was then refluxed at 150 °C for 10 h under an N<sub>2</sub> flow. After cooling to room temperature, the solid was filtered, washed with ethanol, and then dried at 80 °C in vacuo. A white powder of NT-MC was obtained (1.3 g, 3.0 mmol, 50 % yield) by recrystallization from a mixture of chloroform and TFA. The other two MCs (Br-MC and OD-MC in Chart 1) were prepared in a similar manner by the reaction of DBrNT or ODPA and CHA. The yellowish powder of Br-MC was obtained (0.26 g, 0.44 mmol, 60 % yield). The white powder of OD-MC was obtained (0.43 g, 0.91 mmol, 86 % yield). PMMA (0.071 g) was stirred in chloroform (1 mL) for 3 h, and NT-MC (0.00037 g, 0.00086 mmol) was added to the solution, followed by stirring for 1 day. The resulting colorless and transparent solution was spin-coated onto a fused silica substrate, followed by drying at 100 °C for 1 h. Film of Br-MC and OD-MC dispersed in PMMA were also prepared in a similar manner. The weight fractions of the MCs in these films were 1.0 wt%.

## 2.3. Preparation of PI films.



Scheme 2. Synthesis route of N6-PI.



Scheme 1. Synthesis of NT-MC.

The chemical structures of CoPIs, NTDA-6FDA/DCHM (N6-PI), DBrNT-6FDA/DCHM (Br6-PI), NTDA-ODPA/DCHM (NO-PI), and DBrNT-ODPA/DCHM (BrO-PI), are shown in Chart 1. A synthesis scheme of N6-PI film is shown in Scheme 2. A PI precursor, poly(amic acid)silyl ester (PASE), was prepared using the in situ silylation method [31]. DCHM (0.2 g, 0.95 mmol) and BSTFA (0.26 g, 1.0 mmol) were stirred in DMAc (2.6 mL) for 30 min in an ice bath (solution I). NTDA (0.064 g, 0.24 mmol) was stirred in DMAc (0.5 mL) for 30 min in an ice bath (solution II). Solution II was mixed with solution I and stirred for 10 min in an ice bath. 6FDA (0.32 g, 0.71 mmol) was then added to the solution, followed by stirring for 4 h in an ice bath and 2 days at room temperature. The resulting colorless and transparent solution was spin-coated onto a fused silica substrate, followed by soft-baking at 70 °C for 50 min and subsequent one-step thermal imidization procedure; film was gradually heated from 70 to 220 °C at a heating rate of 3.0 °C/min, and kept at the final temperature for 1.5 h under an N<sub>2</sub> flow. Thus, N6-PI film was cooled to room temperature. Br6-PI, NO-PI, and BrO-PI films were prepared in the same manner. The CoPI films were prepared using the same molar ratios of NTDA/DBrNT (25 mol%) to 6FDA and ODPA (75 mol%).

## 2.4. Measurements.

PL excitation/emission spectra were measured with F-7100 luminescence spectrometer (Hitachi Hi-Tech, Japan) equipped with an R928

photomultiplier tube (Hamamatsu Photonics, Japan). Photoluminescence spectra under vacuum conditions were measured using a custom-made vacuum chamber (Akada Industry Co., Ltd, Japan) installed in the same luminescence spectrometer. Spectra were measured after pumping the chamber out using a vacuum pump (Xtradry 150-2, Pfeiffer Vacuum GmbH, Germany), and the inside pressure reached around 10 Pa after pumping for 30 min. Photoluminescence spectra at low temperatures were measured by mounting the samples on a temperature controller (CoolSpek UV USP-203-B, Unisoku Co., Ltd, Japan) installed in the same spectrometer. Samples were cooled by liquid nitrogen supplied from the reservoir into the chamber. Photoluminescence quantum efficiency ( $\Phi_{\text{total}}$ ) was measured by using a calibrated integrating sphere (C9920-02, Hamamatsu Photonics, Japan) connected to a multichannel analyzer (C7473-36, Hamamatsu Photonics, Japan) via an optical fiber link. FL lifetime measurements with a time resolution of less than 1 ns were conducted using a PL lifetime measurement system (Quantaurs-Tau, C11367-24, Hamamatsu Photonics, Japan) at room temperature. The decay component was recorded using excitation by applying a flashing light-emitting diode (LED) at wavelengths of 340 nm and 365 nm. FL decay curves were accumulated until the peak intensity reached 1000 counts. Ph lifetimes were measured using a xenon flash lamp unit (C11567-02, Hamamatsu, Japan). Ph decay curves were recorded under excitation using two bandpass filters (BrightLine 340-12 and 360-12, Semlock Inc., USA) whose transmission ranges were 334-346 nm and 354-366 nm, respectively, and the decay signals were accumulated for 5 min. The emission decay curves were fitted using one to two exponential functions. The average lifetime was calculated as  $\langle \tau \rangle = \frac{\sum A_i \tau_i^2}{\sum A_i \tau_i}$ , where  $A_i$  is the pre-exponential factor for a lifetime  $\tau_i$ .

### 3. Results and discussion

#### 3.1. Optical properties of PMMA-dispersed MCs.

Figure 1 shows the excitation/emission spectra of NT-MC and Br-MC dispersed in PMMA films measured at room temperature (293 K), where  $\lambda_{\text{ex}}$  is the excitation wavelength, and  $\lambda_{\text{em}}$  is the monitoring emission wavelength. Table 1 summarizes the peak wavelengths of excitation and emission spectra ( $\lambda_{\text{exp}}$ ,  $\lambda_{\text{emp}}$ ), Stokes shifts ( $\nu$ ), and PL quantum yields ( $\Phi_{\text{total}}$ ) of the NT-MC and Br-MC films. Figure 2 shows the PL decay curves of the MCs dispersed in

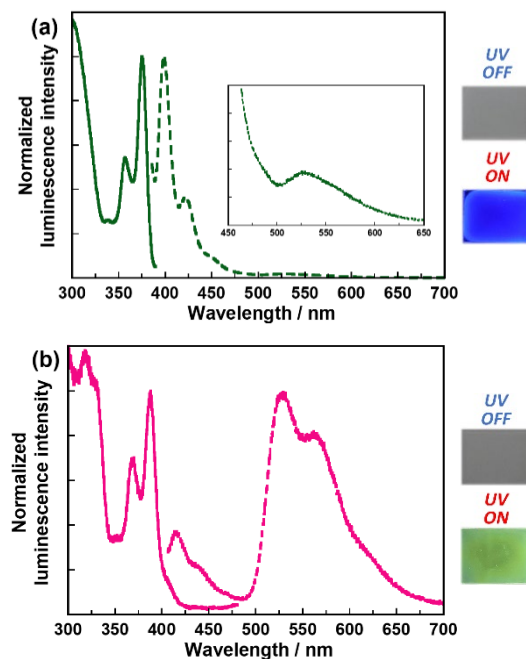


Fig. 1. Excitation (solid line) and emission (dotted line) spectra of (a) NT-MC (Inset: enlarged view of emission spectrum) ( $\lambda_{\text{em}} = 400$ ,  $\lambda_{\text{ex}} = 375$  nm) and (b) Br-MC ( $\lambda_{\text{em}} = 528$ ,  $\lambda_{\text{ex}} = 390$  nm).

PMMA films measured at room temperature in the ambient air and under vacuum conditions. NT-MC exhibits two emission peaks at  $\lambda_{\text{emp}} = 398$  and 526 nm. The former peak is readily attributable to the FL emitted from the locally excited  $\pi$ - $\pi$  transition because the PL measured at 400 nm decayed exponentially with the longest decay component of 5.42 ns under atmospheric condition with oxygen, and its Stokes shift is relatively small ( $\nu = 1541 \text{ cm}^{-1}$ ). By contrast, the latter weak peak is attributable to Ph because the PL measured at 525 nm decayed with the longest decay component of 1.52 s under vacuum condition with a very large  $\nu$  of  $7655 \text{ cm}^{-1}$ .

Br-MC exhibits three emission peaks at  $\lambda_{\text{emp}} = 416$ , 527 and 570 nm. The first one is readily attributable to FL because of the small  $\nu$  value of

Table 1. PL properties of MCs dispersed in PMMA and N6-PI/Br6-PI films.

Sample	$\lambda_{\text{exp}}$ (nm)	$\lambda_{\text{emp}}$ (nm)	$\nu$ ( $\text{cm}^{-1}$ )	$\Phi_{\text{total}}$	
NT-MC	375	398	1541	0.33	
		526	7655		
Br-MC	388	416	1735	0.10	
		527	6798		
N6-PI	376	403	1781	0.20	
		508	6910		
Br6-PI	325	428	2542	0.024	
		386	542		7388
		472			

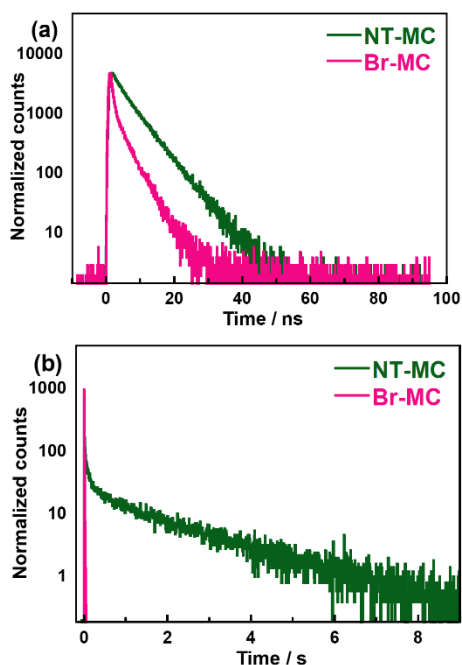


Fig. 2. (a) FI decay curves under atmospheric condition (NT-MC: ( $\lambda_{\text{ex}}$ ,  $\lambda_{\text{em}}$ ) = (365, 400 nm), Br-MC: (405, 415 nm) and (b) Ph decay curves under vacuum condition (NT-MC: ( $\lambda_{\text{ex}}$ ,  $\lambda_{\text{em}}$ ) = (360, 524 nm), Br-MC: (360, 527 nm).

1735  $\text{cm}^{-1}$ , and the PL measured at 415 nm decayed exponentially with the longest decay component of 1.97 ns under vacuum condition. By contrast, the latter two intense peaks are attributable to Ph because of the very large  $\nu$  value of 7698  $\text{cm}^{-1}$  for the second one, and the PL measured at 527 nm decayed with the longest decay component of 4.98 ms under atmospheric condition. The fact that the same decay curves were observed for the second and third peaks indicates that these two peaks originate from the same Ph having different vibration modes. Notably, these are the first observations of the phosphorescence from 2,3,6,7-naphthalene- diimide and its brominated derivative.

The quantum yields of FI and Ph ( $\Phi_f$ ,  $\Phi_p$ ) of NT-MC and Br-MC were estimated from the  $\Phi_{\text{total}}$  value and the peak areas of the FI and Ph of NT-MC and Br-MC, and the  $\Phi$  values thus estimated are listed in Table 2. The  $\Phi_p$  value of Br-MC is significantly larger than that of NT-MC, which indicates that the efficiency of Ph is drastically increased due to the enhancement of ISC by introducing bromine atoms to the naphthalene core of NTDA.

Table 2. PL quantum yields of MCs.

MCs	$\Phi_{\text{total}}$	$\Phi_f$	$\Phi_p$
NT-MC	0.33	0.32	0.01
Br-MC	0.10	0.01	0.09

### 3.2. Optical properties of N6-PI and Br6-PI films.

Figure 3 shows the PL spectra of N6-PI and Br6-PI films measured at room temperature together with those of the MCs. Table 1 also summarizes the estimated values of  $\lambda_{\text{exp}}$ ,  $\lambda_{\text{emp}}$ ,  $\nu$ , and  $\Phi$  for N6-PI and Br6-PI films. Note that each of N6-PI and Br6-PI exhibits a similar shape of emission spectrum of the corresponding MC. It indicates that the copolymerization of NTDA or DBrNT with 6FDA can maintain the inherent PL properties of the naphthalene core imide moieties. Intriguingly, 6FDA effectively enhances the solubility of PASEs in polar solvents, but it does not affect the photophysical processes of the CoPIs derived from NTDA/DBrNT.

As shown in Fig. 4(a), the PL measured at 508, 520 nm for N6-PI decayed exponentially with the longest decay component of 1.77 s at 77 K and 0.647 s under vacuum condition at 293 K. The PL measured at 508 nm of NT-MC also decayed exponentially with the longest decay component of 3.63 s at 77 K. In general, typical Ph lifetime ( $\tau_p$ ) of organic compounds are in the order of  $\mu\text{s}$ – $\text{ms}$ , and  $\tau_p$  longer than 100 ms is called ‘long-lived phosphorescence lifetime’. Thus, the  $\tau_p$ s of NT-MC and N6-PI are readily categorized as very long-lived Ph [32,33]. The molecular mobility restricted by the rigid structure of NTDA moiety effectively reduces the non-radiative deactivation from the excited triplet state. The fact that the decay components of

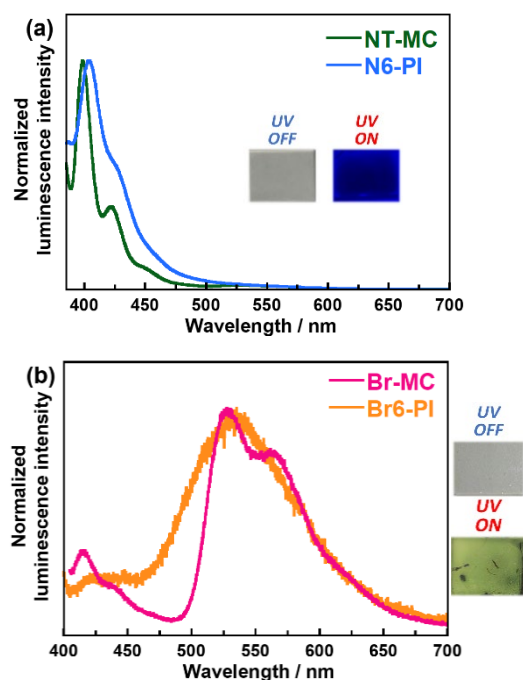


Fig. 3. PL spectra of (a) NT-MC and N6-PI ( $\lambda_{\text{ex}}$  = 375 nm), and (b) Br-MC and Br6-PI ( $\lambda_{\text{ex}}$  = 390 nm) (Inset: photographs of N6-PI and Br6-PI films).

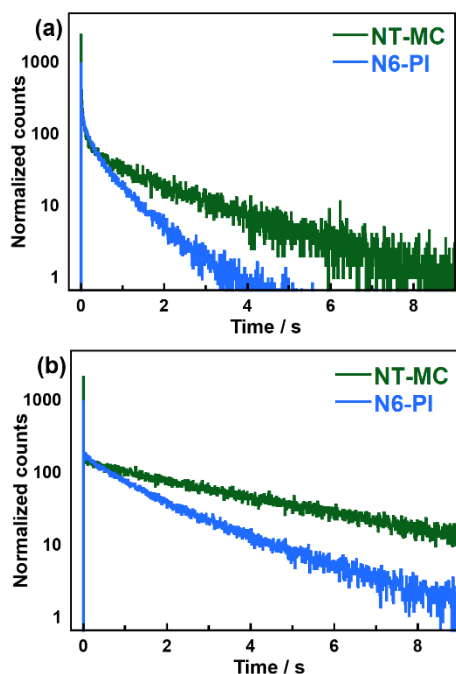


Fig. 4. Ph decay curves (a) measured under vacuum condition at 293 K ( $\lambda_{ex} = 360$  nm, NT-MC:  $\lambda_{em} = 524$  nm, N6-PI:  $\lambda_{em} = 520$  nm) (b) measured at 77 K under nitrogen atmosphere ( $\lambda_{ex} = 360$  nm,  $\lambda_{em} = 508$  nm) of NT-MC and N6-PI.

N6-PI are slightly shorter than those of NT-MC suggests that the local motion of NT-MC molecules dispersed in PMMA is more tightly restricted than the NTDA moieties in N6-PI even at 77 K. In other words, the local motion of PI chain is not completely frozen at this temperature.

### 3.3. Excitation energy transfer between dianhydrides

Figure 5 shows the excitation/emission spectra of OD-MC dispersed in PMMA. OD-MC exhibits an excitation band at 330 nm, which is obviously different from the excitation wavelengths of NT-MC and Br-MC ( $\lambda_{exp} = 375$  nm for NT-MC, and  $\lambda_{exp} = 390$  nm for Br-MC) (Fig. 1). This suggests that

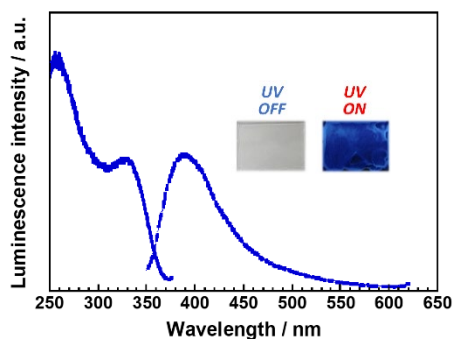


Fig. 5. Excitation (solid line,  $\lambda_{em} = 409$  nm) and emission (dotted line,  $\lambda_{ex} = 340$  nm) spectra of OD-MC dispersed in PMMA.

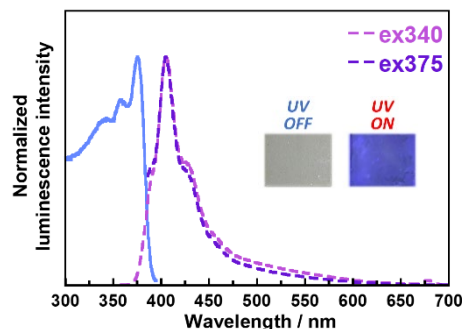


Fig. 6. Excitation (blue solid line,  $\lambda_{em} = 404$  nm) and emission (purple dotted line) spectra of NO-PI excited at 340 and 375 nm.

each composing dianhydride of CoPIs (NTDA/DBrNT and ODPa) could be selectively excited by adjusting the excitation wavelength of UV irradiation.

Figure 6 shows the emission spectra of NO-PI excited at 340 and 375 nm. NO-PI exhibits two emission peaks at  $\lambda_{emp} = 405$  and 570 nm regardless of the excitation wavelength. This clearly indicates that the emissions from NTDA and ODPa moieties cannot be separated in NO-PI by changing the excitation wavelength. As mentioned above, OD-MC exhibits an emission peak at around 400 nm which is close to that of NT-MC. Meanwhile, the PL of OD-MC exhibited a FI lifetime ( $\tau_f$ ) of 5.9 ns and Ph lifetime ( $\tau_p$ ) of 885 ms at 77 K, and these are distinctly different from those of NT-MC ( $\tau_f = 5.42$  ns,  $\tau_p = 3.63$  s). Thereby, the emission process of NO-PI could be analyzed from the PL decay curves observed by the excitation of ODPa moiety at 340 nm and that of NTDA moiety at 360 or 365 nm. In case that the PL is only emitted from the NTDA moiety, the decay curve should be fitted by single component, whereas in case that the PL is emitted from both the NTDA and ODPa moieties, the decay curve could be composed of two components having different slopes, which can be used to characterize the major emitting component in the CoPIs.

Figure 7 shows the FI decay curves of NO-PI excited at 340 and 365 nm and measured at 405 nm, together with the Ph decay curves excited at 340 and 360 nm at 77 K and measured at 570 nm. Both the decay curves show single component decays. Table 3 summarizes the FI and Ph lifetimes ( $\tau_f$ ,  $\tau_p$ ) of NO-PI. The FI lifetimes of the dianhydride moiety in the copolymer should be shorter than those of the homopolymers, though the Ph lifetime of NO-PI are significantly longer than those of ODPa-based homopolyimide ( $\tau_f = 7.0$  ns,  $\tau_p = 619$  ms). These facts suggest that the PL of NO-PI is emitted not

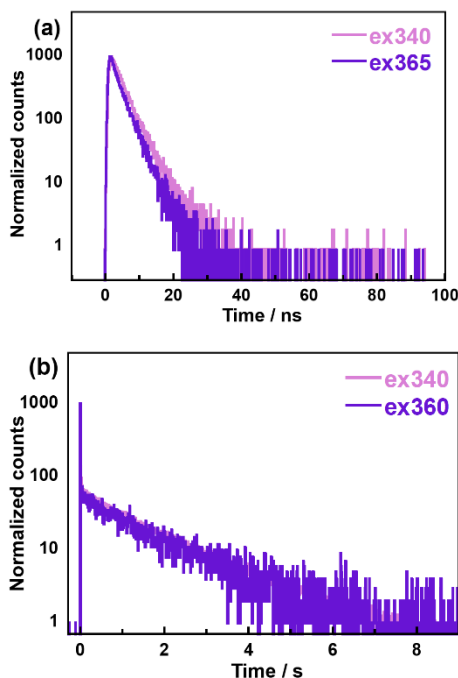


Fig. 7. (a) FI decay curves at room temperature ( $\lambda_{em} = 405$  nm) and (b) Ph decay curves at 77 K ( $\lambda_{em} = 570$  nm) of NO-PI.

from the ODPA moiety but from the NTDA moiety. This is well supported by the fact that the emission lifetimes of NO-PI are close to those of NT-MC. When the ODPA moiety of NO-PI is selectively excited at 340 nm, both the FI and Ph were emitted only from the NTDA moiety. This result indicates that when the ODPA moiety is irradiated by UV light at 340 nm, efficient excitation energy transfer immediately occurs from the ODPA to NTDA moieties, and then the NTDA moiety emits the PL.

In the same manner, Fig. 8 shows the emission spectra for BrO-PI excited at 340 and 390 nm. BrO-PI exhibits two emission peaks at  $\lambda_{emp} = 428$  and 548 nm regardless of the excitation wavelength. The emission peaks of BrO-PI can be separated into those from DBrNT and ODPA moieties because OD-MC and Br-MC exhibited emission peaks at different wavelengths ( $\lambda_{emp} = 398$  nm for OD-MC, and  $\lambda_{emp} = 416$  and 527 nm for Br-MC). BrO-PI exhibits emission peak not at around 400 nm but at around 420 and 520 nm, which suggests that the ODPA moiety in BrO-PI does not emit the major part of PL but the DBrNT moiety emits. When the ODPA moiety of BrO-PI is selectively excited at 340 nm, the FI and Ph of BrO-PI were emitted only from the DBrNT moiety. These facts also indicate that when the ODPA moiety is irradiated at 340 nm, efficient excitation energy transfer immediately occurs from the ODPA to DBrNT moieties, and then the DBrNT moiety emits the PL.

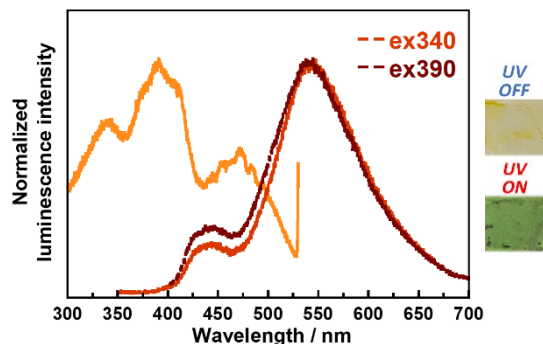


Fig. 8. Excitation (orange solid line,  $\lambda_{em} = 540$  nm) and emission (brown dotted line) spectra of BrO-PI excited at 340 and 390 nm.

Accordingly, these results clearly demonstrate that the copolymerization of NTDA and DBrNT with ODPA having different excitation wavelengths is a facile and versatile method to incorporate and enhance the energy transfer mechanisms in the excited states, which enables to absorb a wide wavelength range of UV light and convert to the useful visible light in the longer wavelength region with desirable efficiency. Moreover, it is

Table 3. FI and Ph lifetimes of NO-PI film.

NO-PI	$\tau_f$ [ns]	$\tau_p$ [s]
ex340	3.64	1.88
ex360/365	3.50	1.87

demonstrated that NO-PI can convert a wide wavelengths range of UV light to long-lived phosphorescence emission through excitation energy transfer, and BrO-PI can convert UV light to room temperature phosphorescence at a longer wavelength of 520 nm. This green light emission is well suited for the spectral response of conventional crystalline Si-type solar cells.

#### 4. Conclusion

The optical absorption and PL properties of three kinds of MCs dispersed in PMMA and four kinds of CoPIs prepared using two dianhydrides containing a rigid naphthalene core (NTDA/DBrNT) were analyzed. It was clarified that copolymerization with 6FDA can maintain the inherent luminescence properties of NTDA/DBrNT moieties. 6FDA endows precursors (PASEs) with excellent solubility without interference in the photophysical processes of NTDA/DBrNT moieties. It was clarified that the restricted molecular mobility by the rigid and planar structures of NTDA and DBrNT moiety reduces the non-radiative deactivation from

the excited states. It was also demonstrated that the CoPIs of NTDA and DBrNT with ODPa having a different excitation wavelength can absorb UV light in a wide wavelength range. When the ODPa moiety in the CoPIs is irradiated at a shorter wavelength of 340 nm, efficient excitation energy transfer occurs from the ODPa to the NTDA/DBrNT moieties, and then bright PL is emitted from the NTDA/DBrNT moieties. In particular, BrO-PI shows Ph emission at a longer wavelength (520 nm) than ODPa-PI. Accordingly, this CoPI film is expected to be applied to wavelength conversion films which absorb a wide range of UV light and readily emit useful and valuable visible light at longer wavelengths which is well suited for the spectral response of crystalline and multi-crystalline Si solar cells.

### References

1. C.E. Sroog, *J. Polym. Sci., Part D Macromol. Rev.*, **11** (1976) 161.
2. D. Creed, C. E. Hoyle, J. W. Jordan, C. A. Pandey, R. Nagarajan, and S. Pankasem, *Macromol. Symp.*, **116** (1997) 1.
3. J. Wakita, H. Sekino, K. Sakai, Y. Urano, and S. Ando, *J. Phys. Chem. B*, **113** (2009) 15212.
4. M. Hasegawa and K. Horie, *Prog. Polym. Sci.*, **26** (2001) 259.
5. K. Takizawa, J. Wakita, K. Sekiguchi, and S. Ando, *Macromolecules*, **45** (2012) 4764.
6. K. Kanosue, T. Shimosaka, J. Wakita, and S. Ando, *Macromolecules*, **48** (2015) 1777.
7. K. Kanosue, R. Augulis, D. Peckus, R. Karpicz, T. Tamulevičius, S. Tamulevičius, V. Gulbinas, and S. Ando, *Macromolecules*, **49** (2016) 1848.
8. K. Kanosue and S. Ando, *Phys. Chem. Chem. Phys.*, **17** (2015) 30659.
9. R. Orita, M. Franckevičius, A. Vyšniauskas, V. Gulbinas, H. Sugiyama, H. Uekusa, K. Kanosue, R. Ishige, and S. Ando, *Phys. Chem. Chem. Phys.*, **20** (2018) 16033.
10. N. Liang, E. Fujiwara, M. Nara, R. Ishige, and S. Ando, *J. Photopolym. Sci. Technol.*, **32** (2019) 449.
11. E. Fujiwara, R. Orita, A. Vyšniauskas, M. Franckevičius, R. Ishige, V. Gulbinas, and S. Ando, *J. Phys. Chem. B*, **125** (2021) 2425.
12. M. Nara, R. Orita, R. Ishige, and S. Ando, *ACS Omega*, **5** (2020) 14831.
13. K. Kanosue, S. Hirata, M. Vacha, R. Augulis, V. Gulbinas, R. Ishige, and S. Ando, *Mater. Chem. Front.*, **3** (2019) 39.
14. K. Kanosue and S. Ando, *ACS Macro Lett.*, **5** (2016) 1301.
15. N. J. Turro, V. Ramamurthy, and J. C. Scaiano, *Angew. Chemie Int. Ed.*, **49** (2009) 6709.
16. H. Shi, Z. An, P.Z. Li, J. Yin, G. Xing, T. He, H. Chen, J. Wang, H. Sun, W. Huang, and Y. Zhao, *Cryst. Growth Des.*, **16** (2016) 808.
17. J. Mei, Y. Huang, and H. Tian, *ACS Appl. Mater. Interfaces*, **10** (2018) 12217.
18. Z. Yang, Z. Mao, X. Zhang, D. Ou, Y. Mu, Y. Zhang, C. Zhao, S. Liu, Z. Chi, J. Xu, Y. C. Wu, P. Y. Lu, A. Lien, and M. R. Bryce, *Angew. Chemie Int. Ed.*, **55** (2016) 2181.
19. R. Reisfeld, *Opt. Mater.*, **32** (2010) 850.
20. S. Hirata, *Adv. Opt. Mater.*, **5** (2017) 1.
21. L. Xiao, Z. Chen, B. Qu, J. Luo, S. Kong, and Q. Gong, *Adv. Mater.*, **23** (2011) 926.
22. V. Gray, D. Dzebo, M. Abrahamsson, B. Albinsson, and K. Moth-Poulsen, *Phys. Chem. Chem. Phys.*, **16** (2014) 10345.
23. Y. Shang, S. Hao, C. Yang, and G. Chen, *Nanomaterials*, **5** (2015) 1782.
24. P. Duan, D. Asthana, T. Nakashima, T. Kawai, N. Yanai, and N. Kimizuka, *Faraday Discuss.*, **196** (2017) 305.
25. S. Guha, M. Chandrasekhar, U. Scherf, and M. Knaapila, *Phys. Status Solidi Basic Res.*, **248** (2011) 1083.
26. S. Guha and M. Chandrasekhar, *Phys. Status Solidi Basic Res.*, **241** (2004) 3318.
27. H. Ma, Q. Peng, Z. An, W. Huang and Z. Shuai, *J. Am. Chem. Soc.*, **141** (2019) 1010.
28. S. Mukherjee and P. Thilagar, *Chem. Commun.*, **51** (2015) 10988.
29. A. Amillo, T. Huld, P. Vourlioti, R. Müller and M. Norton, *Energies*, **8** (2015) 3455.
30. D. Yang, H. Liang, Y. Liu, M. Hou, L. Kan, Y. Yang, and Z. Zang, *Dalt. Trans.*, **49** (2020) 4725.
31. Y. Oishi, K. Ogasawara, H. Hirahara, and K. Mori, *J. Photopolym. Sci. Technol.*, **14** (2001) 37.
32. K. Narushima, Y. Kiyota, T. Mori, S. Hirata, and M. Vacha, *Adv. Mater.*, **31** (2019) 1807268.
33. Y. Su, S.Z.F. Phua, Y. Li, X. Zhou, D. Jana, G. Liu, W.Q. Lim, W.K. Ong, C. Yang, and Y. Zhao, *Sci. Adv.*, **4** (2018) 9732.